Available online at www.sciencedirect.com
ScienceDirect
Journal of Sound and Vibration 304 (2007) 722–734
JOURNAL OF SOUND AND VIBRATION
www.elsevier.com/locate/jsvi

Modal analysis of magneto-electro-elastic plates using the state-vector approach

Jiangyi Chen[a], Hualing Chen[a], E. Pan[b,*], P.R. Heyliger[c]

[a]*School of Mechanical Engineering, Xi'an Jiaotong University, Xi'an 710049, PR China*
[b]*Department of Civil Engineering, University of Akron, OH, USA*
[c]*Department of Civil Engineering, Colorado State University, CO, USA*

Received 19 January 2005; received in revised form 23 February 2007; accepted 9 March 2007
Available online 2 May 2007

Abstract

The state-vector approach is proposed to analyze the free vibration of magneto-electro-elastic laminate plates. The extended displacements and stresses can be divided into the so-called in-plane and out-of-plane variables. Once the state equation for the out-of-plane variables is obtained, a complex boundary value problem is converted into an equivalent simple initial value problem. Through the state equation, the propagator matrix between the top and bottom interfaces of every layer can be easily derived. The global propagator matrix can also be assembled using the continuity conditions. It is obvious that the order of global propagator matrix is not related to the number of layers. Consequently, this approach possesses certain virtues including simple formulation, less expensive computation, etc. To test the formulation, the developed solution is then applied to a simply supported multilayered plate constructed of piezoelectric and/or piezomagnetic materials. The natural frequencies and corresponding mode shapes are computed and compared with existing results. Furthermore, the fundamental modes along with a couple of other higher modes, which have never been reported in previous literature, are presented. Therefore, this completed set of frequencies and mode shapes can be used as benchmarks for future research in this field. It is also believed that the approach could be useful in the analysis and design of smart structures constructed from piezoelectric/piezomagnetic composites.

1. Introduction

The use of bonded and embedded actuators and sensors (piezoelectric and/or piezomagnetic) in structural components is rapidly promoting the development of a new technology of so-called smart materials and structures, which has attracted a great deal of attention in the past few years. For this type of laminated structures, there are many technical challenges in representing the interaction of the magneto-electro-elastic fields. It is well known that the laminated piezoelectric and piezomagnetic materials possess electric-magneto-elastic coupling behaviors. That is, when they undergo elastic deformation, they produce the electric field or magnetic field, and vice versa. Many different approaches have been developed for the analysis of these behaviors for various representative structures. While Heyliger and Saravanos [1] and Gao et al. [2] analyzed

*Corresponding author. Tel.: +1 330 972 6739; fax: +1 330 972 6020.
E-mail address: pan2@uakron.edu (E. Pan).

0022-460X/$ - see front matter © 2007 Elsevier Ltd. All rights reserved.
doi:10.1016/j.jsv.2007.03.021

the free vibration of piezoelectric laminated structures, Cheng et al. [3] and Zhang et al. [4] presented exact solutions for relatively complicated piezoelectric structures under static deformation. Recently Pan [5] derived the exact closed-form solution for the static deformation of a simply supported magneto-electro-elastic layered plate with a new and simple formalism which is based on the pseudo-Stroh formalism and the propagator matrix method. That approach was extended to the analysis of free vibrations of similar layered structures by Pan and Heyliger [6]. More recently, Lage et al. [7] developed a very nice finite element model for the structures made of magneto-electro-elastic materials with complex geometry.

The state-vector approach is a very useful tool for the analysis of laminated structures. Initially the approach was employed in the analysis of purely elastic structures [8–11]. It was then extended to investigate the exact solutions of piezoelectric and/or piezomagnetic structures under static deformation [12–16]. In this approach, the extended displacements and stresses can be divided into the so-called in-plane and out-of-plane variables. Once the state equation for out-of-plane variables is obtained, a complex boundary value problem is converted into an equivalent simple initial value problem. The propagator matrix between the top and bottom interfaces of each layer can be derived easily by solving the state equation. The global propagator matrix can also be assembled using the appropriate continuity conditions between the layers. It is obvious that the order of the global propagator matrix is not related to the number of layers. Consequently, this approach possesses certain advantages, including a simple and concise formulation and less-expensive computation.

In this paper, the equations of motion for magneto-electro-elastic laminate structures are derived by virtue of the state-vector approach. By considering the boundary conditions of a simply supported plate, we express the analytical solution of the equations of motion in the form of an infinite series, and then a simple state equation is obtained. After assembling the propagator matrix for each layer, a very simple equation which directly relates the top and bottom surfaces of the layered plate is derived. With the application of boundary conditions, the natural frequencies and corresponding modal shapes can then be directly obtained by solving the resulting equation.

As a numerical example, we apply our solution method to the sandwich plate made of piezoelectric $BaTiO_3$ and magnetostrictive $CoFe_2O_4$, with four different lay-ups (i.e., B only, F only, B/F/B, and F/B/F, with B standing for $BaTiO_3$ and F for $CoFe_2O_4$). Representative results are presented and compared with those in Ref. [6]. Besides the perfect matches to the available literature results, the fundamental and a couple of higher modes are presented. While the complete set of natural frequencies and modal shapes can serve as benchmarks in future research, the proposed general approach could be useful in the efficient analysis and design of smart structures constructed from piezoelectric/piezomagnetic composites.

2. State space equation

Consider an anisotropic, magneto-electro-elastic, and N-layered rectangular plate with horizontal dimensions L_x and L_y and total thickness H (in the vertical or thickness direction) as shown in Fig. 1. A Cartesian coordinate system is attached to the plate and its origin is at one of the four corners on the bottom surface, with the plate occupying the positive region. Layer j is bonded by the lower interface z_{j-1} and the upper interface z_j with thickness $h_j = z_j - z_{j-1}$. We assume that the extended displacement and traction vectors are continuous across the layer interface. On the top and bottom surfaces of the plate, a combination of traction and/or displacements are assumed to be known. We further assume that its four edges are simply supported, which is consistent with Eq. (18) in the next section.

For a linear, anisotropic magneto-electro-elastic solid, the coupled constitutive equation can be written in the following form:

$$\sigma_i = c_{ik}\gamma_k - e_{ki}E_k - q_{ki}H_k, \quad D_i = e_{ik}\gamma_k + \varepsilon_{ik}E_k + d_{ik}H_k, \quad B_i = q_{ik}\gamma_k + d_{ik}E_k + \mu_{ik}H_k, \tag{1}$$

where σ_i, D_i and B_i are the stress, electric displacement and magnetic induction, respectively; γ_k, E_k and H_k are the strain, electric field and magnetic field, respectively; c_{ik}, ε_{ik} and μ_{ik} are the elastic, dielectric, and magnetic permeability coefficient matrices, respectively; and e_{ik}, q_{ik} and d_{ik} are the piezoelectric, piezomagnetic and magnetoelectric coefficients, respectively. We remark that various uncoupled cases can be reduced by setting the appropriate coefficients to zero, while material coefficients used in this paper are taken from Pan and Heyliger [6] and Ramirez et al. [17].

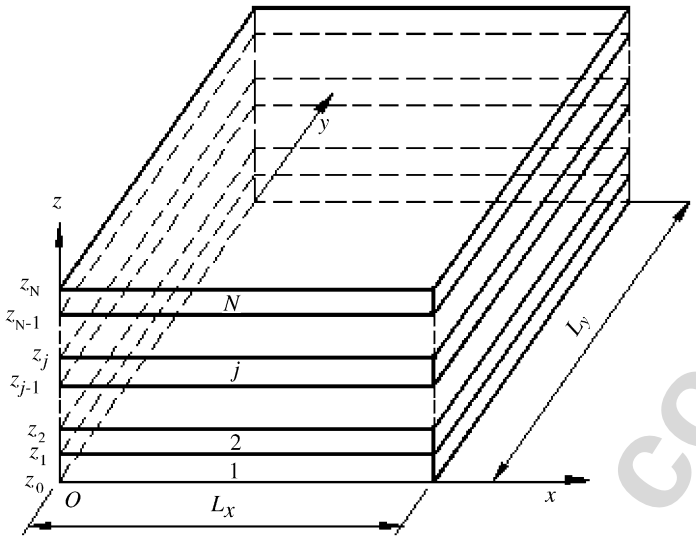

Fig. 1. The magneto-electro-elastic layered plate.

The relationship between strain and displacement, electric (magnetic) field and its potential can be expressed as

$$\gamma_{ij} = 0.5\left(u_{i,j} + u_{j,i}\right), \quad E_i = -\varphi_{,i}, \quad H_i = -\psi_{,i}, \tag{2}$$

where $u_i = [u\ v\ w]^{\mathrm{T}}$ are the elastic displacements, and φ and ψ are the electric and magnetic potentials, respectively. The subscript after the comma, e.g., "$,i$", in the elastic displacement, electric and magnetic potentials denotes partial derivative with respect to the ith component of the coordinates.

For the free vibration problem, the body forces, electric charge and current densities are zero; thus the governing equations of motion for the dynamic case are given by

$$\sigma_{ij,j} = \rho \frac{\partial^2 u_i}{\partial t^2}, \quad D_{j,j} = 0, \quad B_{j,j} = 0, \tag{3}$$

where ρ is the density of the material. Eqs. (1) to (3) form the equation set which includes 17 equations and 17 unknowns. The 17 unknowns are composed of three elastic displacements, six stresses, three electric displacements, three magnetic inductions, one electric potential and one magnetic potential.

To solve the problem conveniently, we will first convert the unknowns into the dimensionless forms, as defined below:

$$\sigma = \sigma/c_{\max}, \quad D = D/e_{\max}, \quad B = B/q_{\max}, \quad s = s/x_{\max}, \quad \varphi = \varphi e_{\max}/c_{\max}, \tag{4}$$

$$\psi = \psi q_{\max}/c_{\max}, \quad \rho = \rho/\rho_{\max}, \quad \omega = \omega x_{\max} \Big/ \sqrt{c_{\max}/\rho_{\max}}, \tag{5}$$

where $c_{\max}$, $e_{\max}$ and $q_{\max}$ are the maximum values of the elastic, piezoelectric and piezomagnetic coefficients of the given materials. Similarly, $x_{\max}$ is the maximum length of the laminate including side lengths and thickness, and $\rho_{\max}$ is the maximum material density among all layers.

The 17 unknowns can be divided into two categories. One is termed in-plane variables (related to the in-plane stress, electrical displacement and magnetic displacement, which are taken as secondary variables). The other is termed out-of-plane variables (related to the extended displacements and tractions, which are taken as primary variables). The primary variables are expressed in the vector form as

$$\boldsymbol{\eta} = \left[u\ v\ D_z\ B_z\ \sigma_z\ \tau_{zx}\ \tau_{zy}\ \varphi\ \psi\ w\right]^{\mathrm{T}}, \tag{6}$$

where the superscript T denotes transpose, subscripts x, y and z correspond to subscripts 1, 2 and 3 in Eqs. (1), (2) and (3). With the state-vector approach, the secondary variables can be easily connected to the primary variables. However, for simplification, only the state equation for the primary variables is considered, which

can be written as

$$\frac{\partial \boldsymbol{\eta}}{\partial z} = \mathbf{A}\boldsymbol{\eta}, \tag{7}$$

where

$$\mathbf{A} = \begin{bmatrix} \mathbf{0} & \mathbf{A}_1 \\ \mathbf{A}_2 & \mathbf{0} \end{bmatrix}, \tag{8}$$

and

$$\mathbf{A}_1 = \begin{bmatrix} a & 0 & \beta_1\dfrac{\partial}{\partial x} & \gamma_1\dfrac{\partial}{\partial x} & -\dfrac{\partial}{\partial x} \\ & b & \beta_4\dfrac{\partial}{\partial y} & \gamma_3\dfrac{\partial}{\partial y} & -\dfrac{\partial}{\partial y} \\ & & \beta_2\dfrac{\partial^2}{\partial x^2}+\beta_5\dfrac{\partial^2}{\partial y^2} & \beta_3\dfrac{\partial^2}{\partial x^2}+\beta_6\dfrac{\partial^2}{\partial y^2} & 0 \\ & \mathbf{Sym} & & \gamma_2\dfrac{\partial^2}{\partial x^2}+\gamma_4\dfrac{\partial^2}{\partial y^2} & 0 \\ & & & & \rho\dfrac{\partial^2}{\partial t^2} \end{bmatrix}. \tag{9}$$

The coefficients in Eq. (9) are

$$\begin{aligned} &a = \frac{1}{c_{55}}, \quad b = \frac{1}{c_{44}}, \quad \beta_1 = -\frac{e_{15}}{c_{55}}, \quad \gamma_1 = -\frac{q_{15}}{c_{55}}, \\ &\beta_2 = \varepsilon_{11} + \frac{e_{15}^2}{c_{55}}, \quad \beta_3 = d_{11} + \frac{e_{15}q_{15}}{c_{55}}, \quad \beta_4 = -\frac{e_{24}}{c_{44}}, \\ &\beta_5 = \varepsilon_{22} + \frac{e_{24}^2}{c_{44}}, \quad \beta_6 = d_{22} + \frac{e_{24}q_{24}}{c_{44}}, \quad \gamma_3 = -\frac{q_{24}}{c_{44}}, \\ &\gamma_2 = \mu_{11} + \frac{q_{15}^2}{c_{55}}, \quad \gamma_4 = \mu_{22} + \frac{q_{24}^2}{c_{44}}. \end{aligned} \tag{10}$$

In Eq. (8), the submatrix $\mathbf{A}_2$ is given as

$$\mathbf{A}_2 = \begin{bmatrix} -\alpha_{11}\dfrac{\partial^2}{\partial x^2} - c_{66}\dfrac{\partial^2}{\partial y^2} + \rho\dfrac{\partial^2}{\partial t^2} & -\alpha_{12}\dfrac{\partial^2}{\partial x\partial y} - c_{66}\dfrac{\partial^2}{\partial x\partial y} & -v_{21}\dfrac{\partial}{\partial x} & -v_{31}\dfrac{\partial}{\partial x} & -v_{11}\dfrac{\partial}{\partial x} \\ & -\alpha_{22}\dfrac{\partial^2}{\partial y^2} - c_{66}\dfrac{\partial^2}{\partial x^2} + \rho\dfrac{\partial^2}{\partial t^2} & -v_{22}\dfrac{\partial}{\partial y} & -v_{32}\dfrac{\partial}{\partial y} & -v_{12}\dfrac{\partial}{\partial y} \\ & & \zeta_{22} & \zeta_{23} & \zeta_{12} \\ & \mathbf{Sym} & & \zeta_{33} & \zeta_{13} \\ & & & & \zeta_{11} \end{bmatrix}, \tag{11}$$

where

$$\alpha_{ij} = c_{ij} - c_{i3}v_{1j} - e_{3i}v_{2j} - q_{3i}v_{3j} \quad (i = 1, 2;\ j = 1, 2), \tag{12}$$

$$v_{ij} = \zeta_{i1}c_{j3} + \zeta_{i2}e_{3j} + \zeta_{i3}q_{3j} \quad (i = 1, 2, 3;\ j = 1, 2), \tag{13}$$

$$\zeta_{ij} = \xi_{ji}/\det\kappa \quad (i = 1, 2, 3;\ j = 1, 2, 3). \tag{14}$$

In Eqs. (13) and (14)

$$\boldsymbol{\kappa} = \begin{bmatrix} c_{33} & e_{33} & q_{33} \\ e_{33} & -\varepsilon_{33} & -d_{33} \\ q_{33} & -d_{33} & -\mu_{33} \end{bmatrix}, \tag{15}$$

and ξ_{ij} are the corresponding algebraic cofactors of $\boldsymbol{\kappa}$.

3. General solution for simply-supported plate

For an extended simply supported multilayered plate, the boundary (edge) conditions can be written as follows:

$$v = w = \varphi = \psi = \sigma_x = 0 \quad \text{at} \quad x = 0 \quad \text{and} \quad x = L_x, \tag{16}$$

$$u = w = \varphi = \psi = \sigma_y = 0 \quad \text{at} \quad y = 0 \quad \text{and} \quad y = L_y. \tag{17}$$

For time-harmonic motion of the form $e^{j\omega t}$($j = \sqrt{-1}$), the general solution of the state variables in the form of $\boldsymbol{\eta}(x, y, z, t) \equiv \tilde{\boldsymbol{\eta}}(x, y, z)e^{j\omega t}$ is expressed as

$$\boldsymbol{\eta}(x, y, t) = \sum_{m=1}^{\infty}\sum_{n=1}^{\infty} \begin{bmatrix} \tilde{u}_{mn}(z)\cos px \sin qy \\ \tilde{v}_{mn}(z)\sin px \cos qy \\ \tilde{D}_{zmn}(z)\sin px \sin qy \\ \tilde{B}_{zmn}(z)\sin px \sin qy \\ \tilde{\sigma}_{zmn}(z)\sin px \sin qy \\ \tilde{\tau}_{zxmn}(z)\cos px \sin qy \\ \tilde{\tau}_{zymn}(z)\sin px \cos qy \\ \tilde{\varphi}_{mn}(z)\sin px \sin qy \\ \tilde{\psi}_{mn}(z)\sin px \sin qy \\ \tilde{w}_{mn}(z)\sin px \sin qy \end{bmatrix} e^{j\omega t}, \tag{18}$$

where ω is the frequency and

$$p = \frac{m\pi}{L_x}, \quad q = \frac{n\pi}{L_y}, \tag{19}$$

with n and m being two positive integers. Substitution of Eq. (18) into the state Eq. (7) then yields

$$\frac{d\tilde{\boldsymbol{\eta}}_{mn}}{dz} = \tilde{\mathbf{A}}(\omega)\tilde{\boldsymbol{\eta}}_{mn}, \tag{20}$$

where

$$\tilde{\boldsymbol{\eta}}_{mn}(z) = \begin{bmatrix} \tilde{u}_{mn} & \tilde{v}_{mn} & \tilde{D}_{zmn} & \tilde{B}_{zmn} & \tilde{\sigma}_{zmn} & \tilde{\tau}_{zxmn} & \tilde{\tau}_{zymn} & \tilde{\varphi}_{mn} & \tilde{\psi}_{mn} & \tilde{w}_{mn} \end{bmatrix}^{T}, \tag{21}$$

$$\tilde{\mathbf{A}}(\omega) = \begin{bmatrix} 0 & \tilde{\mathbf{A}}_1(\omega) \\ \tilde{\mathbf{A}}_2(\omega) & 0 \end{bmatrix}, \tag{22}$$

with

$$\tilde{\mathbf{A}}_1(\omega)=\begin{bmatrix} a & 0 & \beta_1 p & \gamma_1 p & -p \\ 0 & b & \beta_4 q & \gamma_3 q & -q \\ -\beta_1 p & -\beta_4 q & -\beta_2 p^2-\beta_5 q^2 & -\beta_2 p^2-\beta_6 q^2 & 0 \\ -\gamma_1 p & -\gamma_3 q & -\beta_3 p^2-\beta_6 q^2 & -\gamma_2 p^2-\gamma_4 q^2 & 0 \\ p & q & 0 & 0 & -\rho\omega^2 \end{bmatrix}, \tag{23}$$

$$\tilde{\mathbf{A}}_2(\omega)=\begin{bmatrix} \alpha_{11}p^2+c_{66}q^2-\rho\omega^2 & (\alpha_{12}+c_{66})pq & -v_{21}p & -v_{31}p & -v_{11}p \\ (\alpha_{21}+c_{66})pq & \alpha_{22}q^2+c_{66}p^2-\rho\omega^2 & -v_{22}q & -v_{32}q & -v_{12}q \\ v_{21}p & v_{22}q & \zeta_{22} & \zeta_{32} & \zeta_{12} \\ v_{31}p & v_{32}q & \zeta_{23} & \zeta_{33} & \zeta_{13} \\ v_{11}p & v_{12}q & \xi_{21} & \zeta_{31} & \zeta_{11} \end{bmatrix}. \tag{24}$$

The solution of state Eq. (20) can be expressed as follows:

$$\tilde{\boldsymbol{\eta}}_{mn}(z)=\exp\left[\tilde{\mathbf{A}}(\omega)z\right]\tilde{\boldsymbol{\eta}}_{mn}(0)=[\mathbf{P}(z,\omega)]\tilde{\boldsymbol{\eta}}_{mn}(0), \tag{25}$$

which describes the propagating relation between layers. Actually, for the layer j, the state vectors between the top and bottom interfaces of layer j satisfy the following relationship:

$$\tilde{\boldsymbol{\eta}}_{mn}(z_j)=\left[\mathbf{P}_j(h_j,\omega)\right]\tilde{\boldsymbol{\eta}}_{mn}(z_{j-1}). \tag{26}$$

The propagating relationship given in Eq. (26) can be used repeatedly so that we can propagate the physical quantities from the bottom surface to the top surface of the multilayered plate. Thus, we have

$$\tilde{\boldsymbol{\eta}}_{mn}(H)=[\mathbf{T}(\omega)]\tilde{\boldsymbol{\eta}}_{mn}(0), \tag{27}$$

where $[\mathbf{T}(\omega)]=[\mathbf{P}_N(h_N,\omega)][\mathbf{P}_{N-1}(h_{N-1},\omega)]\cdots[\mathbf{P}_2(h_2,\omega)][\mathbf{P}_1(h_1,\omega)]$.

4. Modal analysis

For homogeneous boundary conditions, the natural frequencies and mode shapes can be solved from Eq. (27). Under the assumption that the top and bottom surfaces are free boundaries (i.e., the elastic traction and z-direction electric displacement and magnetic induction are all zero), the state vector on the bottom surface of Eq. (27) can be expressed as a linear combination of five unit vectors. These can be written in the matrix form as

$$\tilde{\boldsymbol{\eta}}'_{mn}(0)=\begin{bmatrix} 1&0&0&0&0&0&0&0&0&0 \\ 0&1&0&0&0&0&0&0&0&0 \\ 0&0&0&0&0&0&0&1&0&0 \\ 0&0&0&0&0&0&0&0&1&0 \\ 0&0&0&0&0&0&0&0&0&1 \end{bmatrix}^{\mathrm{T}}. \tag{28}$$

Substituting Eq. (28) into (27), we obtain

$$\tilde{\boldsymbol{\eta}}'_{mn}(H)=[T(\omega)]\tilde{\boldsymbol{\eta}}'_{mn}(0). \tag{29}$$

The state vector on the top surface can also be expressed as a linear combination of all rows in matrix $\tilde{\boldsymbol{\eta}}'_{mn}(H)$; thus,

$$\tilde{\boldsymbol{\eta}}_{mn}(H)=\tilde{\boldsymbol{\eta}}'_{mn}(H)\mathbf{R}, \tag{30}$$

where $\mathbf{R}=[r_1\ r_2\ r_3\ r_4\ 1]^{\mathrm{T}}$, and r_i $(i=1,2,3,4)$ are the factors of each linear combination. Considering the boundary conditions, the rows from 3 to 6 of the matrix $\tilde{\boldsymbol{\eta}}'_{mn}(H)$ are related to $\mathbf{R}$ by

$$\left[\tilde{\boldsymbol{\eta}}'_{mn}(H)\right]_{3:6}\mathbf{R}=0. \tag{31}$$

The amplitude of the transverse stress in the yz-plane can be expressed as

$$\tilde{\boldsymbol{\tau}}_{yzmn} = \left[\tilde{\boldsymbol{\eta}}'_{mn}(H)\right]_7 \mathbf{R}. \tag{32}$$

Therefore, substituting $\mathbf{R}$, which can be solved from Eqs. (31) and (32), and setting the transverse stress in the yz-plane be zero, we can easily determine the nature frequencies by a Prohl graph or dichotomy from

Table 1
Dimensionless natural frequencies ω_i of sandwiched piezoelectric and/or magnetostrictive plates

Mode	1	2	3	4	5	6	7	8
B only	1.2660	2.3003	4.0111	5.8050	7.2465	9.7703	10.9049	12.9050
F only	1.0181	1.9747	3.3917	4.6118	5.4544	8.2670	8.5661	11.4523
B/F/B	0.9652	1.8556	3.2353	4.4972	5.3786	8.2569	8.5491	10.8845
F/B/F	1.0672	1.9598	3.3879	4.7424	5.8990	8.3331	8.7094	10.3661

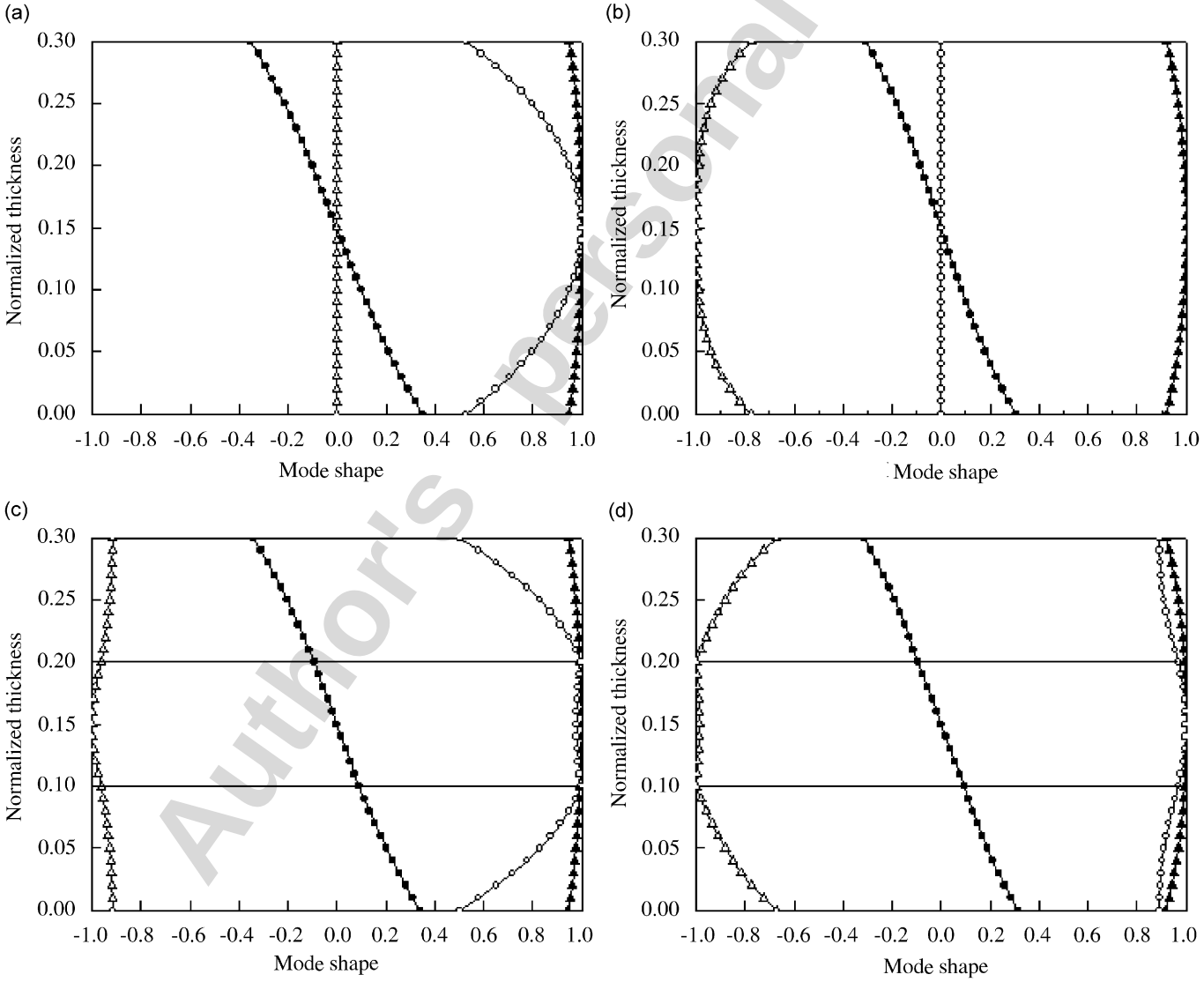

Fig. 2. Anti-symmetric modal shapes of fundamental frequencies in the first column of Table 1: (a) B only with normalized frequency $\omega = 1.2660$; (b) F only with $\omega = 1.0181$; (c) B/F/B with $\omega = 0.9652$; and (d) F/B/F with $\omega = 1.0672$. Solid square for u, solid circle for v, solid triangle for w, open circle for φ, and open triangle for ψ.

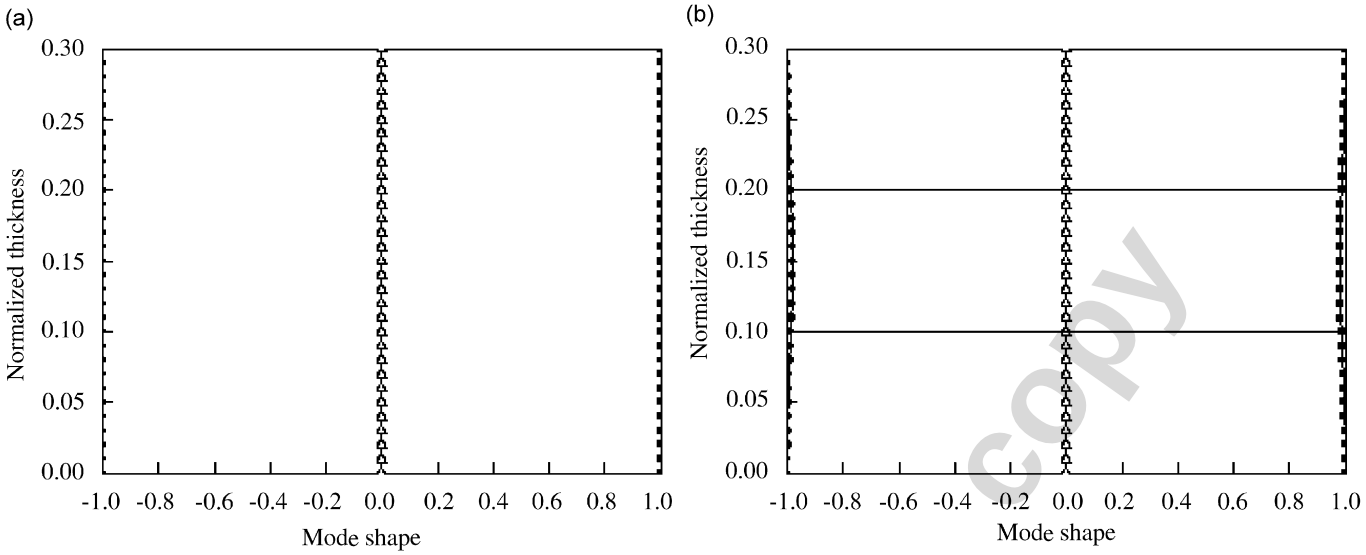

Fig. 3. Symmetric mode shapes of fundamental frequencies in the second column of Table 1: (a) B only with normalized frequency $\omega = 2.3003$; (b) B/F/B with $\omega = 1.8556$. Solid square for u, solid circle for v, solid triangle for w, open circle for φ, and open triangle for ψ.

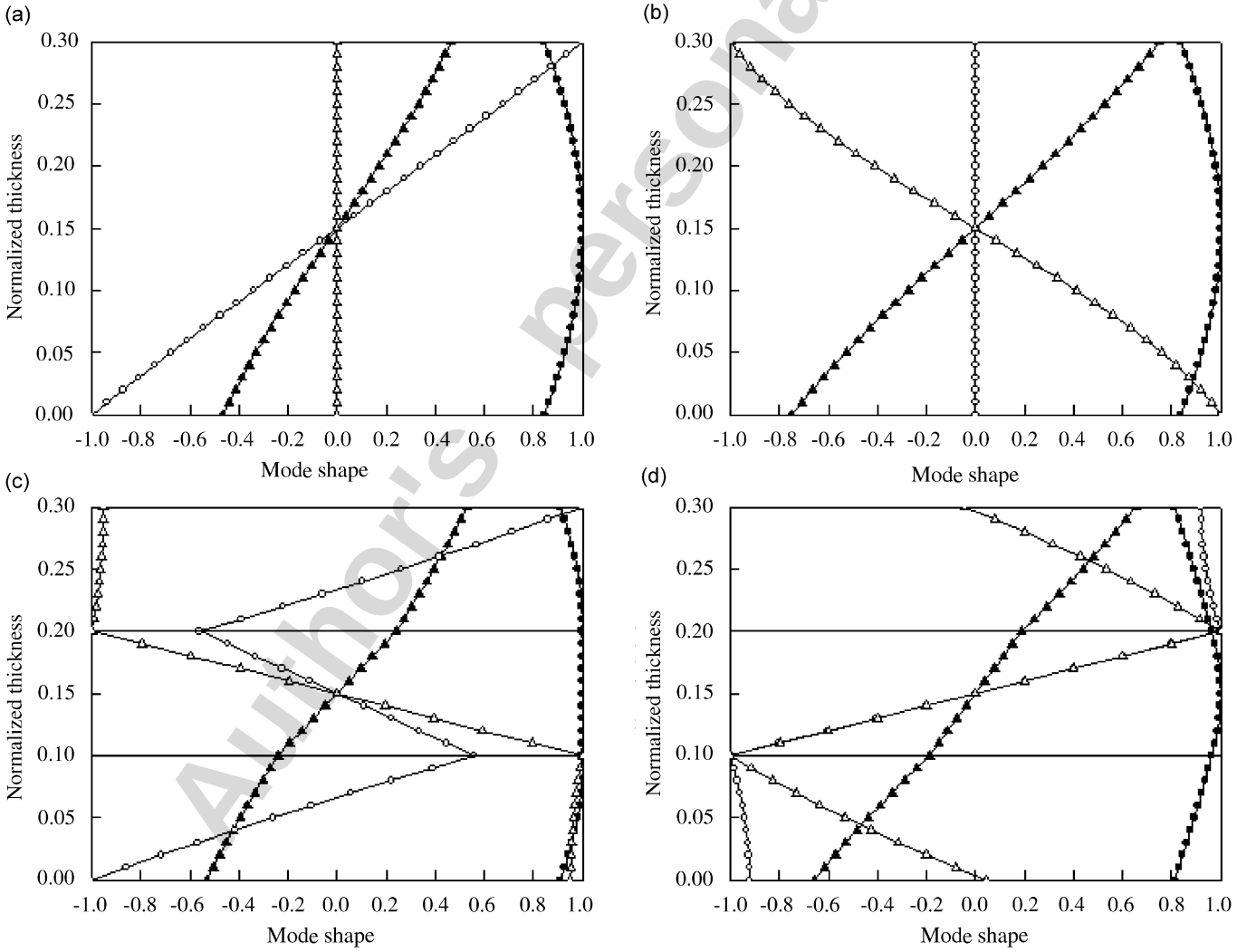

Fig. 4. Symmetric modal shapes of frequencies in the third column of Table 1. (a) B only with normalized frequency $\omega = 4.0111$; (b) F only with $\omega = 3.3917$; (c) B/F/B with $\omega = 3.2353$; and (d) F/B/F with $\omega = 3.3879$. Solid square for u, solid circle for v, solid triangle for w, open circle for φ, and open triangle for ψ.

Eq. (32). Under the assumption that the thickness in the z-direction is divided into K sections, and first letting $\mathbf{\Phi}_0^i = \tilde{\boldsymbol{\eta}}'_{mn}(0)\mathbf{R}$, we obtain

$$\mathbf{\Phi}_L^i = \exp\left[\tilde{\mathbf{A}}(\omega_i)z_L\right]\mathbf{\Phi}_{L-1}^i \quad (L = 1, 2, \ldots K), \tag{33}$$

where ω_i is the ith natural frequency, and z_L is the z-coordinate on the top of section L. Meanwhile, $\mathbf{\Phi}_L^i (L = 0, 1, 2, \ldots K)$ constructs the ith mode shape of the laminated plate. In order to describe the mode shapes of the structure more accurately, the number K is typically taken to be much larger than the number of layers within the plate.

5. Simplification of the propagator matrix

In order to simplify the computational task, we can expand the exponential matrix $e^{\tilde{\mathbf{A}}z}$ in Eq. (25) into an infinite Taylor series as follows:

$$\begin{aligned}\exp\left\{\begin{bmatrix} 0 & \tilde{\mathbf{A}}_1 \\ \tilde{\mathbf{A}}_2 & 0 \end{bmatrix} z\right\} &= \begin{bmatrix} \mathbf{I} & 0 \\ 0 & \mathbf{I} \end{bmatrix} + \begin{bmatrix} 0 & \tilde{\mathbf{A}}_1 \\ \tilde{\mathbf{A}}_2 & 0 \end{bmatrix} z + \frac{z^2}{2!}\begin{bmatrix} 0 & \tilde{\mathbf{A}}_1 \\ \tilde{\mathbf{A}}_2 & 0 \end{bmatrix}\begin{bmatrix} 0 & \tilde{\mathbf{A}}_1 \\ \tilde{\mathbf{A}}_2 & 0 \end{bmatrix} + \frac{z^3}{3!}\begin{bmatrix} 0 & \tilde{\mathbf{A}}_1 \\ \tilde{\mathbf{A}}_2 & 0 \end{bmatrix}\begin{bmatrix} 0 & \tilde{\mathbf{A}}_1 \\ \tilde{\mathbf{A}}_2 & 0 \end{bmatrix}\begin{bmatrix} 0 & \tilde{\mathbf{A}}_1 \\ \tilde{\mathbf{A}}_2 & 0 \end{bmatrix} + \cdots \\ &= \begin{bmatrix} \cosh\left(z\sqrt{\tilde{\mathbf{A}}_1\tilde{\mathbf{A}}_2}\right) & \dfrac{\tilde{\mathbf{A}}_1}{\sqrt{\tilde{\mathbf{A}}_2\tilde{\mathbf{A}}_1}}\sinh\left(z\sqrt{\tilde{\mathbf{A}}_2\tilde{\mathbf{A}}_1}\right) \\ \dfrac{\tilde{\mathbf{A}}_2}{\sqrt{\tilde{\mathbf{A}}_1\tilde{\mathbf{A}}_2}}\sinh\left(z\sqrt{\tilde{\mathbf{A}}_1\tilde{\mathbf{A}}_2}\right) & \cosh\left(z\sqrt{\tilde{\mathbf{A}}_2\tilde{\mathbf{A}}_1}\right) \end{bmatrix}. \end{aligned} \tag{34}$$

By letting $\mathbf{G} = \tilde{\mathbf{A}}_1\tilde{\mathbf{A}}_2$ and $\mathbf{H} = \tilde{\mathbf{A}}_2\tilde{\mathbf{A}}_1$, the exponential matrix is recast as

$$\exp\left\{\begin{bmatrix} 0 & \tilde{\mathbf{A}}_1 \\ \tilde{\mathbf{A}}_2 & 0 \end{bmatrix} z\right\} = \begin{bmatrix} \cosh\left(z\sqrt{\mathbf{G}}\right) & \dfrac{\tilde{\mathbf{A}}_1}{\sqrt{H}}\sinh\left(z\sqrt{\mathbf{H}}\right) \\ \dfrac{\tilde{\mathbf{A}}_2}{\sqrt{\mathbf{G}}}\sinh\left(z\sqrt{\mathbf{G}}\right) & \cosh\left(z\sqrt{\mathbf{H}}\right) \end{bmatrix}. \tag{35}$$

Assuming that the eigenvalues and the corresponding eigenvectors of the matrix $\mathbf{G}$ are, respectively, $\mathbf{\Pi}$ and $\mathbf{\Psi}$, we have

$$\sqrt{\mathbf{G}} = \mathbf{\Psi}\sqrt{\mathbf{\Pi}}\,\mathbf{\Psi}^{-1} \equiv \mathbf{\Psi}\mathbf{\Lambda}\mathbf{\Psi}^{-1} \tag{36}$$

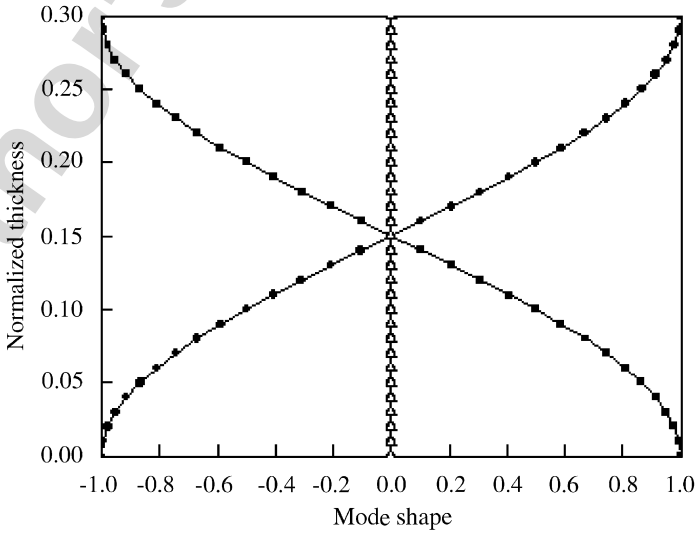

Fig. 5. Anti-symmetric modal shapes of frequencies in the fourth column of Table 1. B only with normalized frequency $\omega = 5.8050$. Solid square for u, solid circle for v, solid triangle for w, open circle for φ, and open triangle for ψ.

and

$$\cosh(z\sqrt{\mathbf{G}}) = \mathbf{I} + \frac{z^2(\mathbf{\Psi\Lambda\Psi}^{-1}\,\mathbf{\Psi\Lambda\Psi}^{-1})}{2!} + \frac{z^4(\mathbf{\Psi\Lambda\Psi}^{-1}\,\mathbf{\Psi\Lambda\Psi}^{-1}\,\mathbf{\Psi\Lambda\Psi}^{-1}\,\mathbf{\Psi\Lambda\Psi}^{-1})}{4!} + \cdots$$
$$= \mathbf{\Psi}\left[\mathbf{I} + \frac{z^2\mathbf{\Lambda}^2}{2!} + \frac{z^4\mathbf{\Lambda}^4}{4!} + \cdots\right]\mathbf{\Psi}^{-1}. \quad (37)$$

Let the eigenvalues of $\mathbf{G}$ be $s_0, s_1, \ldots s_n$, then Eq. (37) can be expressed in a very simple form as

$$\cosh(z\sqrt{\mathbf{G}}) = \mathbf{\Psi}\,\mathrm{diag}\left[\cosh\left(z\sqrt{s_0}\right), \cosh\left(z\sqrt{s_1}\right), \ldots, \cosh\left(z\sqrt{s_n}\right)\right]\mathbf{\Psi}^{-1}. \quad (38)$$

Similar processes can be introduced for the calculation of $\cosh(z\sqrt{\mathbf{H}})$, $\sinh(z\sqrt{\mathbf{G}})/\sqrt{\mathbf{G}}$, and $\sinh(z\sqrt{\mathbf{H}})/\sqrt{\mathbf{H}}$.

6. Numerical examples

In this section, we apply the above formulation to the study of natural frequencies and modal shapes of the three-layered plate. The horizontal dimensions of the plate are ($L_x = L_y = 1$ m), and each layer is composed of

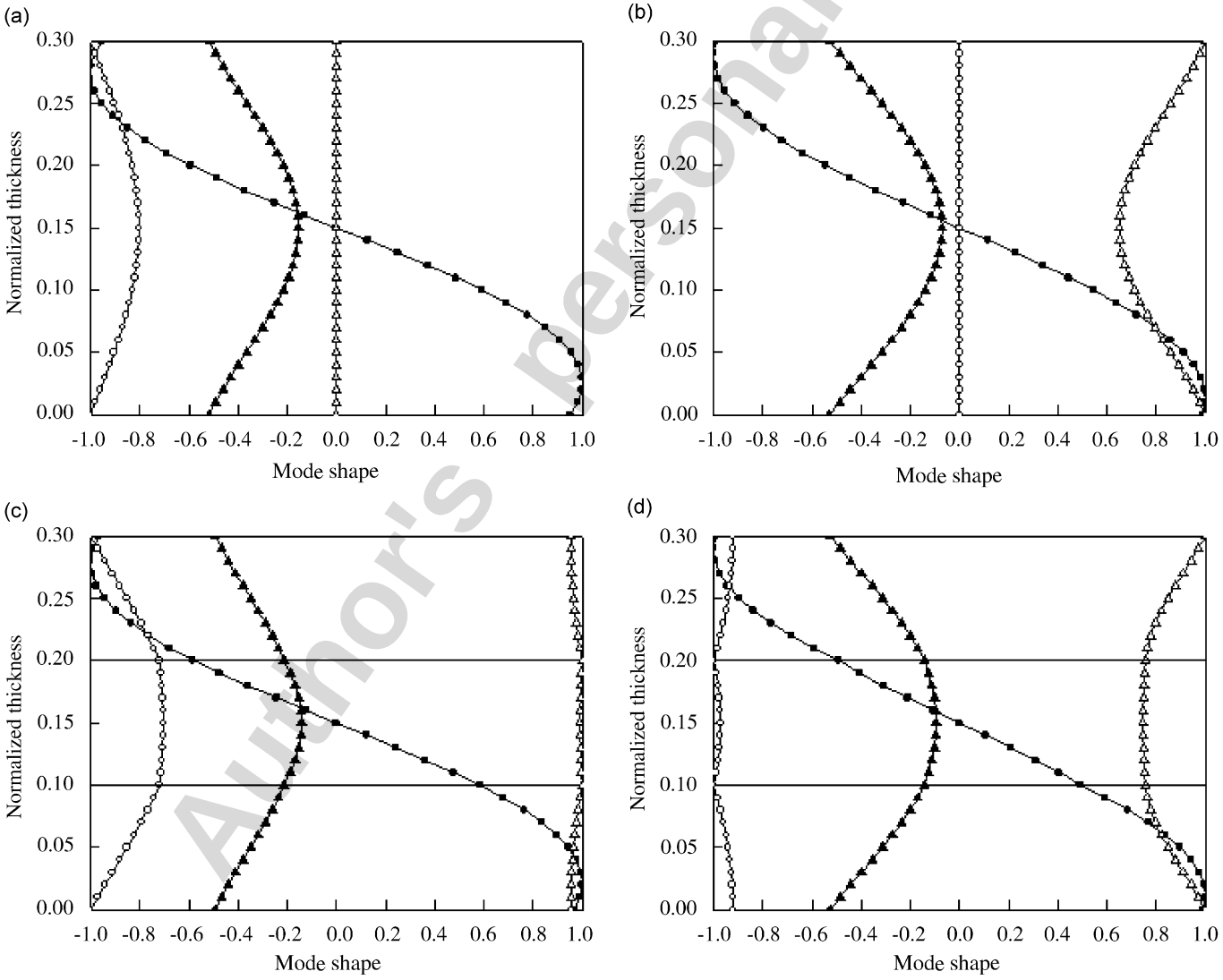

Fig. 6. Anti-symmetric modal shapes of frequencies in the fifth column of Table 1: (a) B only with normalized frequency $\omega = 7.2465$; (b) F only with $\omega = 5.4544$; (c) B/F/B with $\omega = 5.3786$; and (d) F/B/F with $\omega = 5.8990$. Solid square for u, solid circle for v, solid triangle for w, open circle for φ, and open triangle for ψ.

either piezoelectric $BaTiO_3$ or magnetostrictive $CoFe_2O_4$ with material properties from Pan and Heyliger [6] (*Note*: In Ref. [6], the densities for both materials were assumed to be the same, i.e., with $\rho = 5700\,kg/m^3$; in this paper, however, we use the density $\rho = 5800\,kg/m^3$ for $BaTiO_3$ and $5300\,kg/m^3$ for $CoFe_2O_4$ [17]). Furthermore, each layer is assumed to be of equal thickness of 0.1 m so that the total thickness of the plate is $H = 0.3$ m. Four different cases are considered: "B only", "F only", "B/F/B", and "F/B/F", with B standing for $BaTiO_3$ and F for $CoFe_2O_4$. B only represents a homogeneous plate with stack B/B/B, and F only with stack F/F/F. The integers m and n in Eq. (19) for the wavenumbers p and q are fixed at 1. Listed in Table 1 are the first eight natural frequencies in dimensionless form (Eqs. (4) and (5)) for each of the four cases (using the densities in Ref. [17] for B and F), with some of the frequencies for modes 2–5 being slightly different to those available in Ref. [6] due to the difference in the choice of density. However, if both densities are assumed to be equal as they are in Ref. [6], the frequencies corresponding to modes 2–5 are exactly the same as those presented in Pan and Heyliger [6] based on a different approach.

Mode shapes corresponding to the mode frequencies 1–6 in Table 1 are plotted in Figs. 2–7. In these figures, the elastic displacements in the x-, y-, and z-directions are normalized by the maximum value in the whole thickness region for the three components. The electric potential and magnetic potential are normalized by

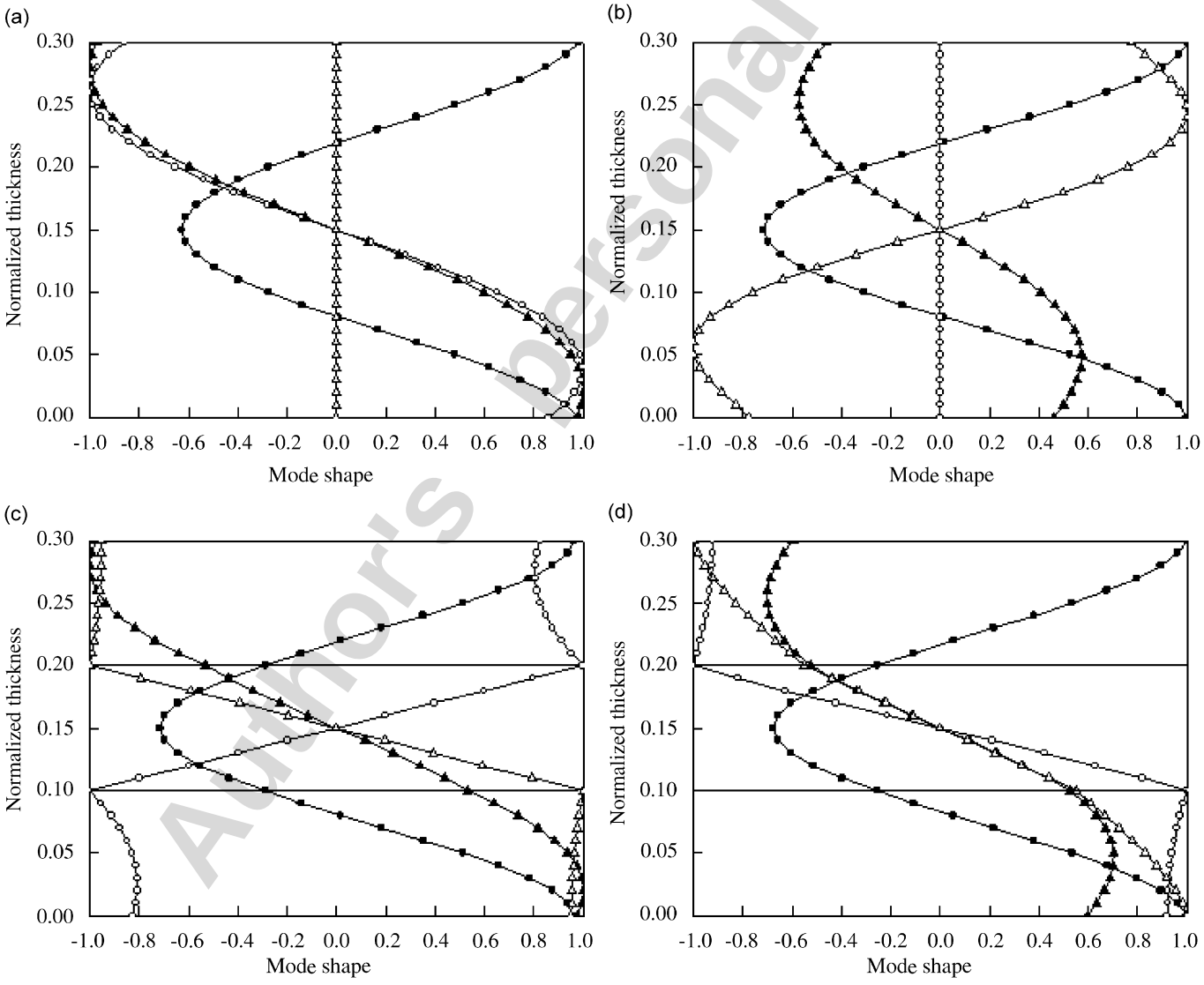

Fig. 7. Symmetric modal shapes of frequencies in the sixth column of Table 1: (a) B only with normalized frequency $\omega = 9.7703$; (b) F only with $\omega = 8.2670$; (c) B/F/B with $\omega = 8.2569$; and (d) F/B/F with $\omega = 8.3331$. Solid square for u, solid circle for v, solid triangle for w, open circle for φ, and open triangle for ψ.

their corresponding maximum (nonzero) values. First, compared to Pan and Heyliger [6], the mode shapes corresponding to modes 2–5 (i.e., Figs. 3–6) are the same as those in Ref. [6] (even though the densities are slightly different). Since these modal shapes have been discussed in detail in Ref. [6], we concentrate on the fundamental and the 6th mode shapes, i.e., which are shown, respectively, in Figs. 2 and 7.

The fundamental mode shapes are shown in Figs. 2a–d for the four different lay-ups. While it is clear that this is an anti-symmetric mode, the three elastic displacement mode shapes are obviously independent of the different lay-ups. In other words, the elastic displacement shape is insensitive to the piezoelectric and/or piezomagnetic coupling. On the other hand, the mode shape of the electric and magnetic potentials, particularly that of the electric potential, are very sensitive to the four different layered cases, and thus could be applied to the inverse of material property and structure lay-ups. Figs. 7a to 7d show the symmetric mode shapes of the 6th mode whose natural frequencies are given in Table 1. Similarly while the elastic displacements are clearly independent of the four material lay-ups, the modal shapes of electric and magnetic potentials are completely different for different material cases.

7. Conclusions

In this paper, the state-vector approach was proposed for the analysis of free vibration of magneto-electro-elastic and layered plates. We selected the out-of-plane variables, which include the extended displacements as well as the z-direction tractions, electric displacement and magnetic induction, as the primary unknowns. In so doing, a state equation was derived and the complex boundary value problem was converted into a simple initial value problem. As a special application, a simply supported multilayered plate is assumed for the modal analysis, with the order of the global propagator matrix being extremely simple and independent of the number of layers. For the given four lay-ups, while some of the natural frequencies and the corresponding mode shapes are in excellent agreement with existing literature results (for the reduced case where the two materials are assumed to have the same density), the fundamental and some higher modes are also presented and discussed in detail. The complete set of the frequencies and modal shapes can serve as benchmarks for future numerical analysis, while the general approach described in this paper could find extensive applications in different areas where smart and adoptive coupled composite structures are involved.

Acknowledgment

This project was supported by the National Nature Science Foundation of PR China under Grant no. 50575172.

References

[1] P.R. Heyliger, D.A. Saravanos, Exact free vibration analysis of laminated plates with embedded piezoelectric layers, *Journal of the Acoustical Society of America* 98 (1995) 1547–1557.
[2] J.X. Gao, Y.P. Shen, J. Wang, Three-dimensional analysis for free vibration of rectangle composite laminates with piezoelectric layers, *Journal of Sound and Vibration* 213 (1998) 383–390.
[3] Z.Q. Cheng, C.W. Lim, S. Kitipronchai, Three-dimensional exact solution for inhomogeneous and laminated piezoelectric plates, *International Journal of Engineering Science* 37 (1999) 1425–1439.
[4] C. Zhang, Y.K. Cheung, S. Di, N. Zhang, The exact solution of coupled thermoelectroelastic behavior of piezoelectric laminates, *Computers and Structures* 80 (2002) 1201–1212.
[5] E. Pan, Exact solution for simply supported and multilayered magneto-electric-elastic plates, *Journal of Applied Mechanics* 68 (2001) 608–618.
[6] E. Pan, P.R. Heyliger, Free vibrations of simply supported and multilayered magneto-electro-elastic plates, *Journal of Sound and Vibration* 252 (2002) 429–442.
[7] R.G. Lage, C.M.M. Soares, C.A.M. Soares, J.N. Reddy, Layerwise partial mixed finite element analysis of magneto-electro-elastic plates, *Computers and Structures* 82 (2004) 1293–1301.
[8] L.Y. Bahar, A state space approach to elasticity, *Journal of The Franklin Institute* 299 (1975) 33–41.
[9] Y.C. Das, N.S.V.K. Rao, A mixed method in elasticity, *Journal of Applied Mechanics* 44 (1977) 51–56.
[10] N.S. Abhyankar, S. Chandrashekara, Concise expressions for the dispersion relations for waves in an infinite isotropic plate, *Mechanics Research Communications* 17 (1990) 409–414.

[11] S. Chandrashekara, U. Santhosh, An efficient solution to the free vibration of thick angle-ply laminate, *International Journal of Solids Structures* 27 (1991) 999–1010.
[12] W.Q. Chen, H.J. Ding, R.Q. Xu, Three-dimensional static analysis of multi-layered piezoelectric hollow spheres via state space method approach, *International Journal of solids structures* 38 (2001) 4921–4936.
[13] J.G. Wang, L.F. Chen, S.S. Fang, State vector approach to analysis of multilayered magneto-electro-elastic plates, *International Journal of Solids and Structures* 40 (2003) 1669–1680.
[14] J.S. Lee, L.Z. Jiang, Exact electroelastic analysis of piezoelectric laminate via state space approach, *International Journal of Solids and Structures* 23 (1996) 977–990.
[15] J.G. Wang, S.S. Fang, L.F. Chen, The state vector methods for space axisymmetric problems in multilayered piezoelectric media, *International Journal of Solids and Structures* 39 (2002) 3959–3970.
[16] Y.M. Wang, J.Q. Tarn, C.K. Hsu, State space approach for stress decay in laminates, *International Journal of Solids and Structures* 37 (2000) 3535–3553.
[17] F. Ramirez, P.R. Heyliger, E. Pan, Free vibration response of two-dimensional magneto-electro-elastic laminated plates, *Journal of Sound and Vibration* 292 (2006) 626–644.